Thermal signatures of nanoscale inhomogeneities and ferroelectric order in $[PbZn_{1/3}Nb_{2/3}O_3]_{1-x}[PbTiO_3]_x$

Makoto Tachibana,[1] Kenta Sasame,[2] Hitoshi Kawaji,[2] Tooru Atake,[2] and Eiji Takayama-Muromachi[1]
[1]*National Institute for Materials Science, Namiki 1-1, Tsukuba, Ibaraki 305-0044, Japan*
[2]*Materials and Structures Laboratory, Tokyo Institute of Technology, 4259 Nagatsuta-cho, Midori-ku, Yokohama 226-8503, Japan*
(Received 29 June 2009; revised manuscript received 24 August 2009; published 29 September 2009)

We present the results of thermal conductivity (κ) and heat-capacity (C_p) measurements for the series of $[PbZn_{1/3}Nb_{2/3}O_3]_{1-x}[PbTiO_3]_x$ (PZN-xPT) single crystals with $0 \leq x \leq 1$. Compared to the prototypical glasslike κ found in $PbMg_{1/3}Nb_{2/3}O_3$ (PMN), PZN shows a suppressed plateau in the temperature dependence of κ. This feature of PZN resembles those of PT-doped PMN and is consistent with the coexistence of polar nanoregions (PNRs) and mesoscopic ferroelectric domains in this relaxor compound. For PT-doped PZN, the systematic behavior of κ and C_p suggests that PNRs persist up to slightly beyond the morphotropic phase boundary at $x \approx 0.1$. The high-temperature C_p data on PZN show a broad ferroelectric anomaly, which gradually transforms to a sharp ferroelectric transition with increasing PT content.

DOI: 10.1103/PhysRevB.80.094115 PACS number(s): 77.84.Dy, 65.40.Ba, 63.50.−x, 66.70.−f

I. INTRODUCTION

Lead-based relaxor ferroelectrics with the perovskite structure, such as $PbMg_{1/3}Nb_{2/3}O_3$ (PMN) and $PbZn_{1/3}Nb_{2/3}O_3$ (PZN), have been the focus of a large number of studies because they exhibit extraordinary dielectric and piezoelectric properties.[1] At very high temperatures, relaxors behave like the paraelectric phase of normal ferroelectrics. However, below the characteristic Burns temperature T_d, which is ~620 K for PMN and ~750 K for PZN,[2] the quenched chemical disorder in relaxors leads to the formation of polar nanoregions (PNRs). The presence of PNRs results in a number of unusual features, including a broad and frequency-dependent peak in the dielectric constant ($T_{max} \sim 265$ and 410 K for PMN and PZN, respectively) and strong damping of several phonon modes in the vibrational dynamics.[3] When doped with the normal ferroelectric $PbTiO_3$ (PT), both PMN and PZN show a huge increase in the piezoelectric constant around the morphotropic phase boundary (MPB), which is a narrow composition region separating the relaxorlike rhombohedral phase from the ferroelectric tetragonal phase. However, due to the presence of structural inhomogeneities in these materials, the microscopic mechanisms behind the enhanced functional properties remain poorly understood.[4]

An interesting feature of relaxors is that their low-temperature thermal properties are similar to those found in glasses or amorphous solids.[5–8] This was made especially clear in the recent study of thermal conductivity (κ) and heat capacity (C_p) for the series of PMN-xPT,[9] in which intricate relationships between the thermal properties and nanoscale inhomogeneities were uncovered. Specifically, the classic glasslike behavior[10,11] is found in PMN, which is a prototypical relaxor compound with a macroscopically cubic structure and a small size (~6 nm) of rhombohedral PNRs.[12] With PT doping up to the MPB, which results in larger PNRs coexisting with sub-μm-sized ferroelectric domains,[13,14] the changes in κ are virtually identical to those found in partially crystallized glasses: the glasslike plateau in the temperature dependence of κ is suppressed with increasing x, indicating enhanced microstrains in the crystal. Meanwhile, the glasslike C_p contributions (a linear T coefficient and large C_p/T^3 peak) remain practically constant up to the MPB, reflecting the presence of PNRs in this region of the phase diagram. For PT doping beyond the MPB, the system is in the ferroelectric tetragonal phase and both κ and C_p gradually recover to the conventional crystalline behavior found in PT. These results[9] clarify the roles of nanoscale structures on the thermal properties of PMN-xPT and suggest that similar measurements will lead to better understanding on the structural inhomogeneities in other relaxor ferroelectrics.

In this paper, we report the κ and C_p of PZN-xPT for $0 \leq x \leq 1$ and examine the evolution of local structures and ferroelectric order in this relaxor ferroelectric system. Although PZN-xPT is usually considered as a close analog of PMN-xPT, there are important differences. PZN has much larger PNRs (~20–40 nm) (Refs. 15 and 16) compared to PMN and various studies report that PZN becomes macroscopically rhombohedral below $T_c \sim 390$ K.[1] Also, the MPB in PZN-xPT is a narrow orthorhombic region located at $0.08 < x < 0.11$,[17] compared to the monoclinic MPB at $0.30 < x < 0.37$ in PMN-xPT.[18] Perhaps due to the proximity of the MPB to $x=0$, there have been fewer systematic studies on PZN-xPT covering wide composition regions. Therefore, thermal measurements on this system will be an interesting approach to study the evolution of local structures, especially through comparison to the previous results on PMN-xPT. Furthermore, in addition to the low-temperature measurements, we also report on C_p up to 873 K for the entire series of PZN-xPT. The results track the development of short- and long-range polar orders for various regions in the phase diagram, showing gradual changes in the behavior from relaxor to conventional ferroelectric with PT doping.

II. EXPERIMENT

Single crystals of PZN-xPT with $x=0$, 0.10, 0.22, 0.45, 0.57, 0.86, 0.93, and 1 were grown by the flux method using growth conditions similar to those reported in Ref. 19. The crystals were mostly in the shape of irregular parallelepiped

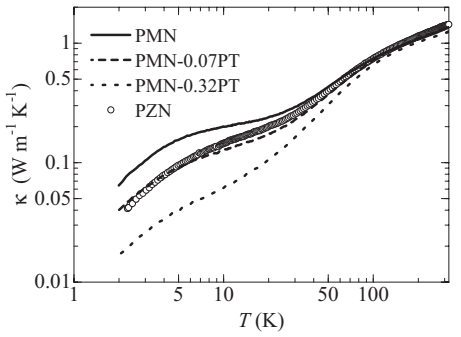

FIG. 1. Thermal conductivities of PMN, PMN-0.07PT, PMN-0.32PT, and PZN crystals. Data for PMN-xPT are reproduced from Ref. 9 and shown as solid, dashed, dotted lines, respectively.

and the compositions were determined by inductively coupled plasma analysis. Powder x-ray diffraction measurements showed no signs of impurity phase and confirmed that the changes in lattice parameters with x are consistent with those reported previously.[20] Thermal conductivity measurements were performed with a Quantum Design PPMS using the thermal transport option. Unlike the PMN-xPT crystals studied in Ref. 9, we could not prepare fully rectangular samples of appropriate dimensions ($\sim 1.5 \times 1.5 \times 3.5$ mm^3) for several compositions in PZN-xPT. Because of the uncertainties ($\lesssim 30\%$) in the geometrical factors, we compare the normalized values $[\kappa(T)/\kappa(300\ \mathrm{K})]$ for PZN-xPT rather than the absolute values. The reproducibility in $\kappa(T)/\kappa(300\ \mathrm{K})$ was checked for several compositions by repeating the measurements on different crystals. For $x=0$, the absolute value shown in this paper corresponds to the average of the results from two rectangular parallelepiped crystals. Heat capacity measurements were performed by two different techniques. Data from 0.6 to 300 K were obtained with a Quantum Design PPMS employing the relaxation method. Data from 300 to 873 K were obtained by the enthalpy method using a Perkin Elmer differential scanning calorimeter. The latter measurements were performed on heating direction under flowing argon. The results were reproducible after the first set of measurements, indicating that the samples did not decompose up to 873 K. The principles of the enthalpy method can be found in Ref. 21.

III. RESULTS AND DISCUSSION

A. Thermal conductivity

We first review the thermal conductivity of PMN-xPT,[9] for which the results on PMN, PMN-0.07PT, and PMN-0.32PT are reproduced in Fig. 1. As mentioned above, the low κ of PMN is both qualitatively and quantitatively identical to the universal behavior found in glasses: the T^2 dependence[5,6] below 1 K (not shown here) is followed by a plateau at ~ 10 K and another increase at higher temperatures. The T^2 behavior arises from the scattering of heat-carrying phonons by a broad distribution of two-level tunneling systems[10,11] and this behavior is also found in a variety of disordered crystals.[22] On the other hand, the distinct glasslike plateau is not widely found among disordered crystals[22] and PMN appears to be a rare example. In PMN, the random distribution of PNRs in the paraelectric matrix is expected to be essential for the classic glasslike behavior. The sensitivity of the glasslike κ to local structures becomes more apparent when the results on PMN-0.07PT and PMN-0.32PT are introduced. For these compositions, PNRs coexist with the oppositely polarized mesoscopic domains and both entities become larger with x.[13,14] Corresponding to these changes in the structure, the plateau is progressively suppressed with PT doping. Remarkably, almost identical behavior is observed in partially crystallized glasses,[23,24] where the suppression is correlated with the concentration of sub-μm-sized crystalline regions. The suppression in glasses has been explained[23,24] with the mismatch of elastic properties at the interface of crystalline and amorphous regions, which gives rise to the thermal boundary resistance[25] with a T^{-3} dependence that suppresses the plateau. Accordingly, the systematic behavior in PMN-xPT can be attributed to an enhanced elastic mismatch, which would occur at the boundaries of mesoscopic ferroelectric domains and those of PNRs embedded in such domains.[26] It should be noted that this type of microstrains has been considered as an important feature of these relaxors, possibly contributing to the large piezoelectric response.[27] Finally, for PT doping beyond the MPB,[9] κ increases and gradually recovers the crystalline behavior; this is consistent with the presence of conventional ferroelectric domains in the tetragonal phase.

The above results on PMN-xPT provide the basis for the present discussion on PZN-xPT. From Fig. 1, we find that the κ of PZN shows a closer resemblance to PMN-0.07PT than to PMN, suggesting that PZN and lightly PT-doped PMN share similarities in their structures. On the small length scale, the presence of PNRs is well known for these compositions and the reported sizes of $\sim 20-40$ nm for PZN (Refs. 15 and 16) and ~ 20 nm for PMN-0.1PT (Ref. 28) are both larger than that in PMN. On the larger length scale, there is some controversy on the average structure of these systems. From conventional x-ray diffraction measurements,[29,30] it was believed that PZN shows a diffuse transition to the rhombohedral phase below 390 K, which is slightly lower than the peak temperature in the dielectric constant. On the other hand, high-energy x-ray diffraction studies[31] found no evidence of rhombohedral distortion down to much lower temperatures. Since the penetration depth of x-rays increases with energy, it was argued that only the surface of PZN crystals shows the rhombohedral distortion, while the inner bulk region remains pseudocubic.[31] However, this was not confirmed in later neutron-diffraction studies,[32,33] which showed clear signs of long-range transition to the rhombohedral structure. Similar conflicts exist in PMN-xPT, where the reported boundary between the cubic and rhombohedral phases varies from $x \sim 0.05$ (Ref. 34) to ~ 0.27 (Ref. 35). Thus, while the origin of these discrepancies remains to be clarified, these studies point to similar structural inhomogeneities in PZN and lightly PT-doped PMN. Because κ is essentially a bulk property, the κ data support the view that the mesoscopic ferroelectric domains are present in the entire region of the crystal.

We now discuss the κ data for the series of PZN-xPT crystals, which are plotted as $\kappa(T)/\kappa(300\ \mathrm{K})$ in Fig. 2. Al-

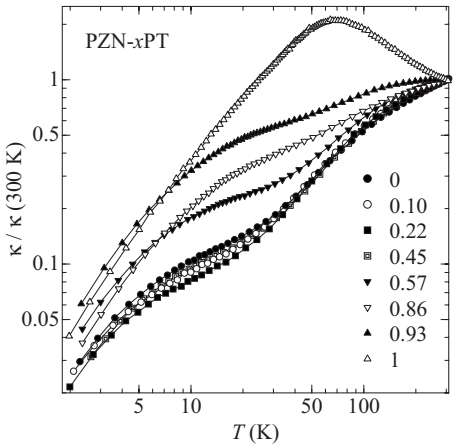

FIG. 2. Thermal conductivity of PZN-xPT single crystals, normalized to the value at 300 K. For clarity, only 1/5 of the total data points are plotted.

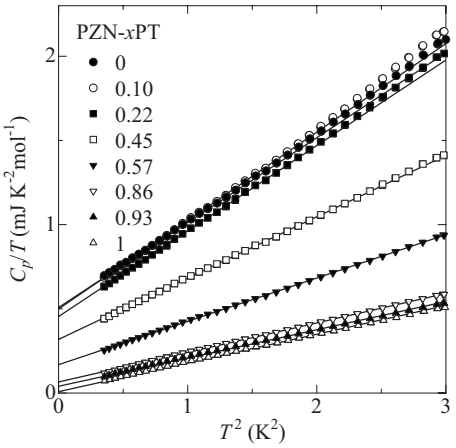

FIG. 3. The low-temperature heat capacity of PZN-xPT plotted as C_p/T vs T^2. The lines are fits to $C_p=\gamma T+\beta T^3$ as described in the text.

though the uncertainties in geometrical factors preclude detailed comparison of the absolute κ values, it is useful to mention that the observed values at 300 K for $0\leq x\leq 0.45$ were clustered between 1.1 and 1.5 W m^{-1} K^{-1}, while successively larger values were found in higher x. (For $x=1$, κ at 300 K is 5.1 W m^{-1} K^{-1}.[8]) Thus, the systematic behavior of real κ for $0\leq x\leq 0.45$ is expected to be similar to that shown in Fig. 2. A close comparison of the $\kappa(T)/\kappa(300\ \mathrm{K})$ data reveals that the plateau shows slight suppression as x is increased from 0 to 0.10 and the strongest suppression occurs at $x=0.22$. For $x\geq 0.22$, the suppression becomes weaker and κ increases with PT doping, which indicate a gradual recovery to the conventional crystalline behavior found in PT.

The successive suppression of the plateau for PT doping up to $x=0.22$ suggests that PNRs persist into the tetragonal phase in PZN-xPT. More specifically, the systematic results from the whole series suggest that the maximum suppression should occur at a certain composition near $x=0.22$, which we locate as the critical composition where PNRs disappear and ferroelectric domains become more conventional with further PT doping. Although previous structural studies on PMN-xPT have provided the notion that PNRs do not persist into the tetragonal phase,[14,28] this appears not to be the case for PZN-xPT: using the neutron pair distribution function (PDF) measurements, Jeong and co-workers[36] found no significant change in the local structure for $0\leq x\leq 0.12$, showing that PNRs can persist beyond the MPB. Similarly, the presence of PNRs was proposed for $x=0.12$ from the acoustic emission measurements,[37] in which the authors argued that PNRs formed at high temperatures should persist below the ferroelectric transition. To better understand the stability limit of PNRs with PT doping, we turn to the low-temperature C_p measurements.

B. Low-temperature heat capacity

The glasslike thermal behavior is also characterized by excess contributions in the low-temperature C_p, which is to be compared to the Debye behavior ($C_p\propto T^3$) of crystalline solids.[10,11] At the lowest temperature region below ~2 K, the heat capacity of glasses follows $C_p=\gamma T+\beta T^3$, where the linear T contribution arises from the two-level tunneling systems and the T^3 contribution is due to phonons. Here, a wide variety of glasses shows a similar value of γ, despite great differences in their chemical compositions. Also, the coefficient β in glasses is much larger than the value expected from the sound velocity, indicating that localized vibrational modes coexist with long-wavelength acoustic phonons. At higher temperatures, glasses show a broad peak in C_p/T^3 near 10 K, which is much larger in height and located at lower temperatures than those found in crystals. In PMN-xPT,[9] these features of glasslike C_p remain virtually constant for PT doping up to the MPB, above which C_p is progressively reduced to the conventional crystalline behavior found in PT. Therefore, these observations in PMN-xPT lead to the important conclusions that (1) the presence of PNRs is essential for the glasslike saturated density of thermal excitations and (2) although not as large as the glasslike value, the quenched chemical disorder in the tetragonal phase also enhances C_p above the Debye behavior. These results provide useful background for the present discussion on PZN-xPT, which is described next. To facilitate the comparison to PMN-xPT, we perform the same sets of analysis as reported in Ref. 9.

The C_p data below 1.8 K for the series of PZN-xPT crystals are shown in Fig. 3, plotted as C_p/T vs T^2. For each composition, the linear behavior at the lowest temperatures indicates that $C_p=\gamma T+\beta T^3$, with the intercept and slope corresponding to γ and β, respectively. For PZN, the best fit to the data gives $\gamma=0.51$ mJ K^{-2} mol^{-1} and $\beta=5.0\times 10^{-4}$ J K^{-2} mol^{-1}, which are similar to those found in PMN.[8,9] The γ value corresponds to the two-level density of states $D(\epsilon)=6.3\times 10^{21}$ states eV^{-1} cm^{-3}, which is within the range found in glasses.[10] From β, the Debye temperature Θ_D can be calculated through $\beta=N(12/5)\pi^4 R\Theta_D^{-3}$, where $R=8.314$ J K^{-1} mol^{-1} and N can be 5 or 1 in perovskites. $N=5$ corresponds to the usual definition of full 15 oscillator strength per formula unit (n_D) and yields $\Theta_D=270$ K, whereas $N=1$ corresponds to $n_D=3$ and gives $\Theta_D=160$ K.

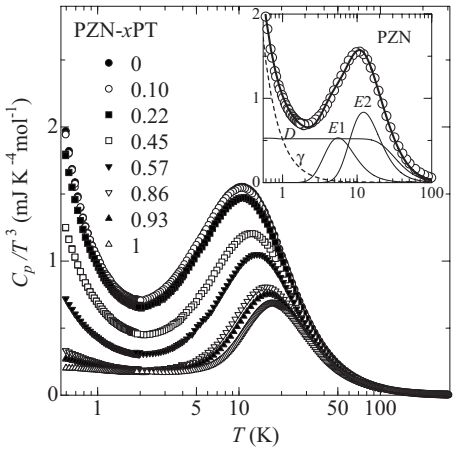

FIG. 4. Heat capacity of PZN-xPT plotted as C_p/T^3 vs T. Data for $x=0$ are almost indistinguishable from those of $x=0.10$ in this plot. Inset shows the result of the fit for $x=0$, including the contributions from the linear term (γ, dashed line), Debye function D, and two Einstein functions $E1$ and $E2$. Only selected data points are shown in the inset for clarity.

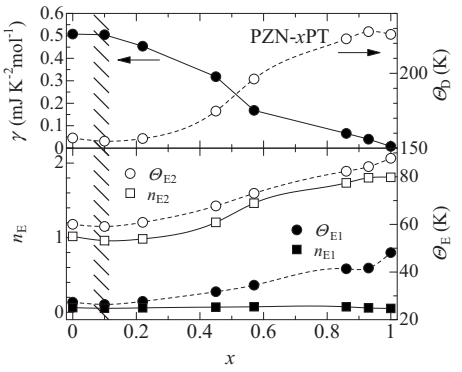

FIG. 5. The x dependence of thermal parameters for PZN-xPT. (Top) the linear C_p coefficient γ and Debye temperature Θ_D and (bottom) the temperatures Θ_E and oscillation strengths n_E of the two Einstein modes. For Θ_D, the oscillator strength n_D was fixed to 3; Θ_D for $n_D=15$ can be obtained by multiplying the present values by $5^{1/3}$. The hatched region represents the morphotropic phase boundary.

These Θ_D values are similar to those reported for PMN.[8,9] In PMN, the thermal Θ_D is much lower than the elastic Θ_D obtained from the sound velocity,[38,39] signifying the presence of nonacoustic phonon contributions to βT^3. Although we are not aware of elastic Θ_D for PZN,[40] the similarity in thermal Θ_D to PMN suggests that this compound also contains glasslike nonacoustic contributions. In PZN-xPT, there is no remarkable change in the low-temperature C_p when x is increased from $x=0$ to 0.10. On the other hand, both γ and β steadily decrease for larger x, in a manner similar to the tetragonal phase of PMN-xPT.[9] As already discussed in the previous studies,[8,9] $x=1$ (PT) shows no contribution from γT and the thermal Θ_D is very close to the elastic Θ_D value.

Figure 4 shows the C_p data plotted as C_p/T^3 over a wide temperature region. In this plot, the linear T term becomes a sharp upturn below 2 K, whereas the T^3 contribution becomes a constant. In addition to these features, a broad peak is observed in each x. As in PMN-xPT,[9] the peak remains almost constant in the relaxor side of the MPB and becomes lower in height and shifts to higher temperatures in the tetragonal phase. The shape of the peak suggests that it can be represented by a combination of Einstein functions, which correspond to localized or dispersionless modes in the lattice dynamics. Accordingly, we first subtract the γT component from the total C_p, and the remaining C_p from 0.6 to 100 K are fitted by a combination of two Einstein functions and a single Debye function. Here, the Einstein function is

$$C_E = n_E R \frac{(\Theta_E/T)^2 e^{\Theta_E/T}}{(e^{\Theta_E/T}-1)^2}$$

and the Debye function is

$$C_D = \frac{3n_D R}{(\Theta_D/T)^3}\int_0^{\Theta_D/T}\frac{x^4 e^x}{(e^x-1)^2}dx.$$

The fitting parameters of the Einstein functions are the characteristic temperatures Θ_{E1} and Θ_{E2} and the oscillator strengths n_{E1} and n_{E2} per formula unit, respectively. To set Θ_D in the Debye function equal to the value obtained from β, its oscillator strength n_D is fixed to 3. The result of the fit and the individual contributions in the C_p/T^3 plot are shown for PZN in the inset of Fig. 4. Similar quality of the fit was obtained in other compositions.

The parameters obtained from the fits are plotted as a function of x in Fig. 5. The results for PZN are very similar to those of PMN,[9] indicating that these compounds share similar low-energy phonon density of states. The parameters remain almost constant as x is increased from 0 to 0.10, which is consistent with the presence of PNRs in these compositions. For $x \geq 0.22$, the parameters deviate from the constant behavior and change continuously up to $x=1$, signaling a gradual recovery to the conventional Debye behavior.[9] Therefore, the C_p data show that the saturated density of glasslike excitations is terminated at a critical composition located within $0.10 \leq x < 0.22$, which is expected to be the maximum PT concentration with PNRs in PZN-xPT. This is fully consistent with the results of κ and we can now deduce that the critical composition (i.e., the maximum suppression of κ) should occur at $0.10 < x < 0.22$ in the tetragonal phase.

Any attempt to understand the microscopic origin of glasslike behavior in relaxors is frustrated by the fact that there is remarkably little such understanding for glasses in general. Nevertheless, the systematic behavior in the thermal properties for PMN-xPT provided strong indications that PNRs are at the heart of glasslike behavior in relaxor systems and from this idea we were able to explain the results on PZN-xPT in a consistent manner. In relaxors, it is possible to assume that different configurational states of PNRs are separated from each other by a broad distribution of potential barriers.[42] If the energy barriers between some of the potentials approach zero, PNRs can provide the physical basis for the two-level tunneling centers. Furthermore, since the configurational dynamics of PNRs is localized, these potentials are also expected to be responsible for the thermal excitations that lead to the excess contributions in βT^3 and the large peak in C_p/T^3. It should be noted that this is basically

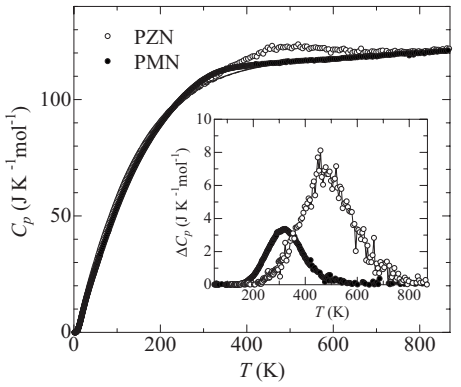

FIG. 6. Heat capacity of PMN and PZN up to 873 K. For PMN, data below 420 K were obtained with an adiabatic calorimeter and reproduced from Ref. 45, whereas data above 420 K were obtained by the enthalpy method (Ref. 46). For PZN, data obtained by the relaxation and enthalpy methods are used below and above 300 K, respectively. The solid and dashed lines, which overlap with each other, are the estimated backgrounds for PZN and PMN, respectively. Inset shows the excess contribution ΔC_p for PMN and PZN. For PMN, the result is slightly different from Ref. 45 due to the different background used in this study.

the situation envisaged by the phenomenological soft potential model,[43] and relaxors may be an important example where the source of glasslike properties can be clearly identified. As phonon-dispersion relations in relaxors can be studied in detail,[3] further insights into the origin of the glasslike behavior are expected from additional studies on the lattice dynamics. In this context, the recent observations[44] of strong coupling between acoustic phonons and PNRs are extremely encouraging.

C. High-temperature heat capacity

While the low-temperature C_p measurements probe the density of low-energy excitations, high-temperature C_p data provide thermodynamic signatures for the formation of PNRs and ferroelectric order in relaxor ferroelectric systems. Previously, Moriya *et al.*[45] reported precise C_p measurements up to 420 K for PMN and PMT (T=Ta) using adiabatic calorimetry. The result on PMN is reproduced in Fig. 6, which also includes unpublished data[46] up to 873 K obtained by the enthalpy method. Except for the unusual curvature of the C_p around 300 K, there is no obvious anomaly over the entire temperature region. In Ref. 45, a clear anomaly was revealed when the data were plotted as effective Debye temperature vs temperature, and the excess contribution ΔC_p was obtained after the background was estimated and subtracted from the total C_p. In Fig. 6, a different background (shown with a dashed line) was obtained by fitting a polynomial function at temperatures well away from the anomaly and the resultant ΔC_p is plotted in the inset. Although this ΔC_p is slightly smaller than that reported in Ref. 45, the consistency in the shape of the peak supports the previous conclusion that ΔC_p tracks the nucleation and growth of PNRs. Especially, ΔC_p starts slightly below $T_d \sim 620$ K where PNRs first appear, and shows a peak at ~320 K

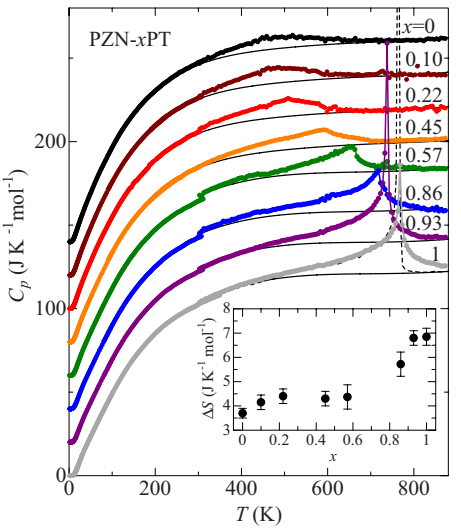

FIG. 7. (Color online) Heat capacity of PZN-xPT up to 873 K. For clarity, data have been successively offset by 20 J K^{-1} mol^{-1}. Dashed line corresponds to the data from a polycrystalline sample of PT (reproduced from Ref. 50), with a peak value of 407 J K^{-1} mol^{-1} at 764 K. Solid lines are the estimated background for each x, obtained by the method described in the text. Small steps in the data at 300 K are due to the change in instrument at this temperature. Inset shows the entropy of the excess contribution ΔS for each composition.

where the size and concentration of PNRs begin to increase rapidly.[12,47] The entropy under the anomaly (ΔS) is 1.9 J K^{-1} mol^{-1}, which is lower than the previous value.[45]

Also shown in Fig. 6 is the C_p of PZN, which was obtained by the relaxation method up to 300 K and by the enthalpy method at higher temperatures. At the highest temperature region, PMN and PZN show almost identical behavior. This is consistent with both compounds being in the cubic paraelectric phase, where C_p is dominated by phonon contributions and approaches the classical Dulong-Petit value of 125 J K^{-1} mol^{-1}. The estimated background for PZN, shown as a solid line in the figure, is very close to that of PMN above 350 K. The resultant ΔC_p is plotted in the inset. Corresponding to $T_d \sim 750$ K in PZN, ΔC_p starts to increase below this temperature region. The peak occurs at ~460 K and is much larger than that of PMN. ΔS is 3.7 J K^{-1} mol^{-1} for PZN, which is almost twice as large as that of PMN. The larger C_p anomaly in PZN can be attributed to the greater degree of ferroelectric order, and this is seen in the structural studies as larger PNRs (Refs. 15 and 16) and macroscopic ferroelectric distortion.[32,33] The absence of a sharp peak in C_p is consistent with the view that the transition occurs through a progressive transformation of PNRs into mesoscopic ferroelectric domains,[29,30] with some PNRs persisting through the transition and coexisting with the long-range polar order. We do not observe any significant feature in ΔC_p at $T^* \sim 500$ K, where several studies have shown evidence for a crossover from dynamic to static character of PNRs.[37,48]

Figure 7 shows the C_p of PZN-xPT in the entire temperature region. Based on the phase diagram of PZN-xPT,[17] x =0.10 undergoes a cubic to tetragonal transition at ~450 K

and a tetragonal to orthorhombic transition at ~300 K. There is a peak in C_p at 460 K due to the former transition, while the observation of the latter transition could be hindered by the change in instrumentation at 300 K. We note the absence of spiky peaks in C_p, which have been reported for the successive ferroelectric transitions in PMN-0.295PT.[49] The difference may be explained by the influence of electrothermal history on ΔC_p; to test this possibility, heat-capacity measurements on electrically poled crystals of $x=0$ and 0.10 are in progress. For $x \geq 0.22$ in the tetragonal side of the MPB, the anomaly in C_p becomes gradually sharper and the peak moves to higher temperatures with increasing x. The ferroelectric transition temperatures are consistent with the published phase diagram.[20] For $x=1$ (PT), our previous result on a polycrystalline sample[50] is also shown with a dashed line. The polycrystalline sample shows a sharp peak at 764 K, with a small tail on the high-temperature side. In comparison, the single crystal shows a smaller peak at 768 K and a larger tail on the high-temperature side, which suggest a larger concentration of growth strains or impurities in the single crystals.

To clarify the anomalous contributions to C_p, we have estimated the baselines as shown in Fig. 7 with solid lines. For $x=1$, the normal regions in the polycrystalline data were used to obtain a polynomial function for the baseline. For the intermediate x, we first obtained smooth lines which are weighted averages of the baselines from $x=0$ and 1. Then, these lines were scaled by less than 5% in the T and C_p axes to establish the baseline for each composition. It is clear that the broad excess contributions above the peak temperature, which correspond to the growth of PNRs in PZN, are also present in the tetragonal compositions for x up to ~0.45. For these compositions, the shape of C_p suggests that the ferroelectric transition does not occur through conventional critical fluctuations in the paraelectric phase. Instead, it is likely that PNRs are formed above the transition, which are then completely merged into ferroelectric domains below the transition. It should be noted that similar observation has been reported in the Brillouin scattering study on PMN-0.55PT,[51] which provided dynamic evidence for PNRs above the ferroelectric transition.

When the baselines are used to obtain ΔS for each composition, the results shown in the inset are obtained. For $x=1$, ΔS from the polycrystalline and single-crystal samples are identical within the error bar. Although the absolute values of ΔS are subject to the usual concern about the choice of baseline, the overall systematic behavior is likely to be intrinsic: for a wide composition region in the tetragonal phase, ΔS remains significantly below the value found in PT. Interestingly, similar behavior is observed for the spontaneous polarization, where the reported values[20] of ~30 μC cm^{-2} for $0.2 \leq x \leq 0.5$ are well below that of PT (~60–70 μC cm^{-2} at room temperature[52]). This is an interesting point that deserves to be further investigated, especially in connection with the quenched chemical disorder present in the tetragonal phase of PZN-xPT.

IV. SUMMARY

In this paper, we have presented the evolutions of κ and C_p for the series of PZN-xPT single crystals, and discussed the similarities and differences to those reported for PMN-xPT. Compared to the prototypical glasslike κ found in PMN, the glasslike plateau is clearly suppressed in PZN. This is similar to the case of PT-doped PMN, and in both cases the suppression can be explained by an enhanced elastic mismatch arising from the coexistence of PNRs and mesoscopic ferroelectric domains in the crystal. In PZN-xPT, the combined results from κ and C_p suggest that PNRs disappear below $x=0.22$ in the tetragonal phase. The C_p measurements up to 873 K on PZN show a broad anomaly due to the diffuse development of ferroelectric order, which is much larger than the corresponding anomaly found in PMN. The peak in C_p becomes gradually sharper with increasing x, without showing any abrupt change across the MPB. As a final note, an interesting result of the thermal measurements is the slow recovery to the conventional ferroelectric and crystalline behavior for PT doping beyond the MPB. This is a clear sign of strong chemical disorder in the tetragonal phase, the presence of which should also affect other physical properties.

ACKNOWLEDGMENTS

We thank Y. Moriya for giving us permission to use the unpublished data on PMN and S. Takenouchi for performing the composition analysis of the crystals. This study was supported by a Grant-in-Aid from JSPS under Grant No. 20740178 and WPI Research Center Initiative on Materials Nanoarchitectonics from MEXT, Japan.

[1] A. A. Bokov and Z.-G. Ye, J. Mater. Sci. **41**, 31 (2006).
[2] G. Burns and F. H. Dacol, Solid State Commun. **48**, 853 (1983).
[3] K. Hirota, S. Wakimoto, and D. E. Cox, J. Phys. Soc. Jpn. **75**, 111006 (2006).
[4] M. Davis, J. Electroceram. **19**, 23 (2007).
[5] D. A. Ackerman, D. Moy, R. C. Potter, A. C. Anderson, and W. N. Lawless, Phys. Rev. B **23**, 3886 (1981).
[6] J. J. De Yoreo, R. O. Pohl, and G. Burns, Phys. Rev. B **32**, 5780 (1985).
[7] M. Tachibana, H. Kawaji, and T. Atake, Phys. Rev. B **70**, 064103 (2004).
[8] M. Tachibana, T. Kolodiazhnyi, and E. Takayama-Muromachi, Appl. Phys. Lett. **93**, 092902 (2008).
[9] M. Tachibana and E. Takayama-Muromachi, Phys. Rev. B **79**, 100104(R) (2009).
[10] *Amorphous Solids: Low Temperature Properties*, edited by W. A. Phillips (Springer, Berlin, 1981).
[11] *Tunneling Systems in Amorphous and Crystalline Solids*, edited by P. Esquinazi (Springer, Berlin, 1998).
[12] I.-K. Jeong, T. W. Darling, J. K. Lee, T. Proffen, R. H. Heffner,

J. S. Park, K. S. Hong, W. Dmowski, and T. Egami, Phys. Rev. Lett. **94**, 147602 (2005).
[13] V. V. Shvartsman and A. L. Kholkin, Phys. Rev. B **69**, 014102 (2004).
[14] F. Bai, J. Li, and D. Viehland, Appl. Phys. Lett. **85**, 2313 (2004); J. Appl. Phys. **97**, 054103 (2005).
[15] D. La-Orauttapong, J. Toulouse, J. L. Robertson, and Z.-G. Ye, Phys. Rev. B **64**, 212101 (2001).
[16] C. Stock, R. J. Birgeneau, S. Wakimoto, J. S. Gardner, W. Chen, Z.-G. Ye, and G. Shirane, Phys. Rev. B **69**, 094104 (2004).
[17] D. La-Orauttapong, B. Noheda, Z.-G. Ye, P. M. Gehring, J. Toulouse, D. E. Cox, and G. Shirane, Phys. Rev. B **65**, 144101 (2002).
[18] B. Noheda, D. E. Cox, G. Shirane, J. Gao, and Z. G. Ye, Phys. Rev. B **66**, 054104 (2002).
[19] L. Zhang, M. Dong, and Z.-G. Ye, Mater. Sci. Eng., B **78**, 96 (2000).
[20] S. Nomura, T. Takahashi, and Y. Yokomizo, J. Phys. Soc. Jpn. **27**, 262 (1969).
[21] S. C. Mraw, in *Specific Heat of Solids*, edited by C. Y. Ho (Hemisphere, New York, 1988).
[22] D. G. Cahill, S. K. Watson, and R. O. Pohl, Phys. Rev. B **46**, 6131 (1992).
[23] C. L. Choy and D. Greig, J. Phys. C **8**, 3121 (1975).
[24] B. Hanna and R. G. Bohn, J. Am. Ceram. Soc. **74**, 3035 (1991).
[25] E. T. Swartz and R. O. Pohl, Rev. Mod. Phys. **61**, 605 (1989).
[26] The boundaries of PNRs in a cubic matrix, as occurs in PMN, are expected to have a much weaker elastic mismatch. See Ref. 31 for a related discussion.
[27] G. Xu, Z. Zhong, Y. Bing, Z.-G. Ye, and G. Shirane, Nature Mater. **5**, 134 (2006).
[28] M. Matsuura, K. Hirota, P. M. Gehring, Z.-G. Ye, W. Chen, and G. Shirane, Phys. Rev. B **74**, 144107 (2006).
[29] A. Lebon, H. Dammak, G. Calvarin, and I. O. Ahmedou, J. Phys.: Condens. Matter **14**, 7035 (2002).
[30] Y.-H. Bing, A. A. Bokov, Z.-G. Ye, B. Noheda, and G. Shirane, J. Phys.: Condens. Matter **17**, 2493 (2005).
[31] G. Xu, Z. Zhong, Y. Bing, Z.-G. Ye, C. Stock, and G. Shirane, Phys. Rev. B **67**, 104102 (2003); **70**, 064107 (2004).
[32] E. H. Kisi and J. S. Forrester, J. Phys.: Condens. Matter **17**, L381 (2005).
[33] J. S. Forrester, E. H. Kisi, K. S. Knight, and C. J. Howard, J. Phys.: Condens. Matter **18**, L233 (2006).
[34] Z.-G. Ye, Y. Bing, J. Gao, A. A. Bokov, P. Stephens, B. Noheda, and G. Shirane, Phys. Rev. B **67**, 104104 (2003).
[35] G. Xu, D. Viehland, J. F. Li, P. M. Gehring, and G. Shirane, Phys. Rev. B **68**, 212410 (2003).
[36] I.-K. Jeong, J. K. Lee, and R. H. Heffner, Appl. Phys. Lett. **92**, 172911 (2008); I.-K. Jeong, Phys. Rev. B **79**, 052101 (2009).
[37] M. Roth, E. Mojaev, E. Dul'kin, P. Gemeiner, and B. Dkhil, Phys. Rev. Lett. **98**, 265701 (2007); E. Dul'kin, M. Roth, P.-E. Janolin, and B. Dkhil, Phys. Rev. B **73**, 012102 (2006).
[38] A. Y. Wu and R. J. Sladek, Phys. Rev. B **27**, 2089 (1983).
[39] G. A. Smolenskii, N. K. Yusin, S. I. Smirnov, and G. Gulyamov, Sov. Phys. Solid State **28**, 522 (1986).
[40] Elastic Θ_D=330 K(n_D=15) and 190 K(n_D=3) can be obtained from the high-temperature ($T \approx 400$ K) sound velocity data in Ref. 41. Higher elastic Θ_D values are expected from $T \rightarrow 0$ K data which can be directly compared to the thermal Θ_D values.
[41] Y. Gorouya, Y. Tsujimi, M. Iwata, and T. Yagi, Appl. Phys. Lett. **83**, 1358 (2003).
[42] B. E. Vugmeister and H. Rabitz, Phys. Rev. B **57**, 7581 (1998); B. E. Vugmeister, *ibid.* **73**, 174117 (2006).
[43] L. Gil, M. A. Ramos, A. Bringer, and U. Buchenau, Phys. Rev. Lett. **70**, 182 (1993).
[44] G. Xu, J. Wen, C. Stock, and P. M. Gehring, Nature Mater. **7**, 562 (2008).
[45] Y. Moriya, H. Kawaji, T. Tojo, and T. Atake, Phys. Rev. Lett. **90**, 205901 (2003).
[46] Y. Moriya, H. Kawaji, and T. Atake (unpublished).
[47] G. Xu, G. Shirane, J. R. D. Copley, and P. M. Gehring, Phys. Rev. B **69**, 064112 (2004).
[48] J. Toulouse, Ferroelectrics **369**, 203 (2008).
[49] Z. Kutnjak, J. Petzelt, and R. Blinc, Nature (London) **441**, 956 (2006); Z. Kutnjak, Ferroelectrics **369**, 198 (2008).
[50] T. Yoshida, Y. Moriya, T. Tojo, H. Kawaji, T. Atake, and Y. Kuroiwa, J. Therm. Anal. Calorim. **95**, 675 (2009).
[51] J.-H. Ko, S. Kojima, A. A. Bokov, and Z.-G. Ye, Appl. Phys. Lett. **91**, 252909 (2007).
[52] M. E. Lines and A. M. Glass, *Principles and Applications of Ferroelectrics and Related Materials* (Clarendon, Oxford, 1977).